Oral Microbiology Immunology 2005: 20: 122–127
Printed in Singapore. All rights reserved

Oral Microbiology and Immunology

Mutational analysis of the *adcCBA* genes in *Streptococcus gordonii* biofilm formation

K. Mitrakul, C. Y. Loo, C. Gyurko, C. V. Hughes, N. Ganeshkumar
Department of Pediatric Dentistry, Goldman School of Dental Medicine, Boston University, Boston, MA, USA

Mitrakul K, Loo CY, Gyurko C, Hughes CV, Ganeshkumar N. Mutational analysis of the adcCBA *genes in* Streptococcus gordonii *biofilm formation.*
Oral Microbiol Immunol 2005: 20: 122–127. © Blackwell Munksgaard, 2005.

Streptococcus gordonii, a primary colonizer, is part of the pioneer biofilm consortium that initiates dental plaque development on tooth surfaces. An insertion of Tn*917-lac* transposon into the *adcR* gene produced a biofilm-defective phenotype. *S. gordonii adcR* is a regulatory gene and is part of an operon (*adc*) that includes three other genes, *adcCBA*. AdcC contains a putative consensus-binding site for adenosine triphosphate, AdcB is a putative hydrophobic membrane protein, and AdcA is a putative lipoprotein permease. Mutants were constructed by insertional inactivation in each of the three *adcCBA* genes and their effects on biofilm formation examined. The *adcC*::*spec*^{R} and *adcB*::*spec*^{R} mutations displayed a biofilm-defective phenotype, whereas the *adcA*::*spec*^{R} mutant was biofilm-positive in a static polystyrene microtiter plate biofilm assay. All three mutants formed poor biofilms in a flow-cell system and were competence-defective, suggesting the *adc* operon plays an important role in *S. gordonii* biofilm formation and competence.

Key words: *adc* operon; biofilm; dental plaque; *Streptococcus gordonii*; streptococci; Tn*917*

N. Ganeshkumar, Department of Pediatric Dentistry, Goldman School of Dental Medicine, Boston University, 801 Albany Street, Room 215, Boston, MA 02118, USA
Tel.: +1 617 638 4773;
fax: +1 617 638 5033;
e-mail: nganesh@bu.edu
Accepted for publication November 4, 2004

Pioneer oral streptococci initiate the formation of oral biofilms on surfaces of teeth by forming mono-species biofilms (22). This is followed by adhesion of other oral bacteria. Growth of these consortia into structured, matrix-embedded, complex microbial communities on the tooth surface results in mature biofilms referred to as dental plaque (3). The growth of these multilayered, dental biofilm communities, their eventual dispersal, and their spread all require the coordinated expression of genes that are finely tuned to various environmental cues such as pH, oxygen tension, and nutrient availability. There is increasing recognition that bacteria growing as biofilms are the major cause of several persistent and chronic bacterial infections that display enhanced resistance to conventional antibiotic therapy and host immune responses (8). The development of a mature biofilm is the result of the expression of phenotypes in sessile growth that are different from the phenotypes expressed by planktonic cells (7, 26). The identification and characterization of various environmental signals that are important to biofilm formation may facilitate the development of alternative strategies to control biofilms.

Trace elements are essential to several cellular processes, play a crucial role in cellular events and participate in bacterial differentiation and growth (12, 13). Biofilm development by the opportunistic pathogen *Pseudomonas aeruginosa* on mucosal surfaces in humans is affected by iron chelators, which inactivate lactoferrin, a component of innate immunity (25). Furanosyl borate diester is an autoinducer 2, a family of related molecules that elicit responses in numerous bacteria species, allowing bacterial populations to coordinate gene expression in a variety of developmental processes. This indicates a potential role for boron in bacterial differentiation (5). Biofilm formation of *Mycobacterium avium* on plastic surfaces is dependent on the presence of the divalent cations, calcium, magnesium, or zinc (4). Mutations affecting the copper-transport genes in *Streptococcus mutans* (28, 29) and in *Streptococcus gordonii* (21) appear to affect biofilm detachment to polystyrene surfaces.

S. gordonii, an early colonizer of tooth surfaces, was used previously to identify genes that are involved in biofilm formation to abiotic surfaces (17–20). A biofilm-defective mutant isolated was found to have a Tn*917-lac* transposon insertion into the *adcR* gene, which was shown to be involved in biofilm formation and competence (19). The *adc* operon in *S. gordonii* consists of four open reading frames (ORFs) – *adcR, adcC, adcB,* and *adcA* – and is

homologous to the zinc regulons in other bacteria (9, 24). Like other metal uptake systems, the *adc* operon also appears to play a role in manganese acquisition (19). In this study, mutations were generated in the *adcCBA* genes and their effect on *S. gordonii* biofilm formation was examined.

Methods

Bacteria, media and chemicals

S. gordonii Challis 2 (17), *S. gordonii adcR*::Tn*917-lac* and *S. gordonii adcR*::*spec*^{R} (19) were subcultured and maintained routinely on Brain Heart Infusion (BHI) agar (BBL, Becton Dickinson, Cockeysville, MD) or Todd Hewitt Broth (Difco Laboratories, Detroit, MI) supplemented with 0.2% yeast extract (THBYE) at 37°C under anaerobic conditions (CO_2/H_2/N_2, 5 : 5 : 90; VWRbrand anaerobic chamber, VWR, Plainfield, NJ). The antibiotic spectinomycin (1 mg/ml) was added when required.

All chemicals were purchased from Sigma (St. Louis, MO) or Fisher Scientific (Pittsburgh, PA). All enzymes for DNA manipulations were purchased from Promega (Madison, WI) or Fisher Scientific unless stated otherwise. Oligonucleotide primers were from Invitrogen Life Technologies (Rockville, MD).

Mutagenesis of the *adc* operon in *S. gordonii*

Polymerase chain reaction (PCR) ligation mutagenesis with vectorless intermediates (15) was used to construct deletion mutants in various ORFs present in *S. gordonii adc* operon (19). The plasmid pSF152 containing a spectinomycin resistance gene, *spec*^{R} (27), was used as the template for amplifying *spec*^{R}.

Initially, PCR amplification of the two flanking regions and the antibiotic marker insert was performed with appropriate primers that incorporated restriction sites of *Mlu*I and *Xba*I, respectively. After electrophoresis on a 1% agarose gel to confirm amplification, the PCR products were purified using the QIAquick PCR Purification Kit (Qiagen, Valencia, CA). The purified PCR products of the 5′ and 3′ flanking fragments were digested with *Mlu*I and *Xba*I, respectively, while the amplified *spec*^{R} cassette was digested with both enzymes. The digested fragments were purified using the QIAquick Nucleotide Removal Kit (Qiagen) and directional ligation was performed at room temperature for 18 h after mixing together the 5′ flanking fragment, the 3′ flanking fragment, and the spectinomycin resistance cassette (18–20).

After ligation, 4 μg of the ligated DNA was used for transformation of *S. gordonii* Challis 2 by the method described previously (17). Transformants were then plated on BHI agar containing spectinomycin and incubated at 37°C anaerobically for 2–5 days. Competence of *S. gordonii* Challis 2 strain and the mutants were assessed by transformation with 4 μg of the ligated DNA and enumerating the colony forming units on solid media containing the appropriate antibiotics. Experiments were done in triplicate.

Reverse Transcription-PCR (RT-PCR)

RT-PCR was performed using RNA from *S. gordonii* Challis 2, *adcC*::*spec*^{R}, and *adcB*::*spec*^{R}mutants to confirm that the mutants generated were nonpolar. Total RNA was extracted from cells grown to mid-log phase [absorbance at 660 nm (A_{600nm}) of 0.3–0.4] using a Qiagen RNeasy mini kit (Qiagen). RT-PCR was performed using RNA isolated from *S. gordonii adcC*::*spec*^{R} with primers adcC P3 (CGT CTA GAC GCA AAA AGT ATG CCG ACC G) and adcA P2 (CGA CGC GTC GAG AAT ACA CTC AGT AAA CCA) spanning the *adcC* to *adcA* region, and using RNA from *S. gordonii adcB*::*spec*^{R} with primers adcA for 1 (CTT GGT GGC TTG TTC CAA TCA GAA AAA A) and adcA rev 2 (AGC ATT TCT TGG GCA ATT TCT TGA CCA G), which span *adcA* under conditions described previously (19, 20). *S. gordonii* Challis 2 RNA was used as a control for RT-PCR with identical primer pairs. The locations of the primers used are shown in Fig. 1A.

Growth assays

The growth rates of *S. gordonii* Challis 2, *adcR*::*spec*^{R}, *adcC*::*spec*^{R}, *adcB*::*spec*^{R} and *adcA*::*spec*^{R} mutants were assessed by inoculating the strains from an overnight THBYE culture into fresh 10 ml THBYE and growing them at 37°C under anaerobic conditions. Growth was quantified by recording the A_{600nm} over 24 h.

Biofilm assays

An *in vitro* microtiter plate biofilm formation assay was performed as previously described (17) using a minimal, defined medium as the biofilm medium. In addition to the microtiter plate biofilm assay, biofilm formation on borosilicate glass coverslips was visualized directly using phase-contrast microscopy (19, 20).

In addition, biofilm formation was also assessed in a flow-cell system (18, 23) and visualized by confocal scanning laser microscopy. A glass flow-cell (BioSurface Technologies Corp., Bozeman, Montana) was used. The substratum consisted of a microscope glass coverslip. An 250 μl volume inoculum was introduced (2×10^7 cells) and was allowed to bind to the surface by inverting the flow cell for 15 min without flow, after which biofilm medium was pumped through the flow-cell channel at a rate of 200 μl per minute. After bacteria were grown in the flow-cell at 37°C for 18 h, confocal scanning laser microscopy was used to examine the spatial organization of the biofilm formed *in situ*. After staining with LIVE/DEAD *bac*Light™ Bacterial Viability Stain according to the manufacturer's instructions (Molecular Probes, Eugene, OR), cells were visualized with a X20 air objective using a Leica TCS SP2 confocal

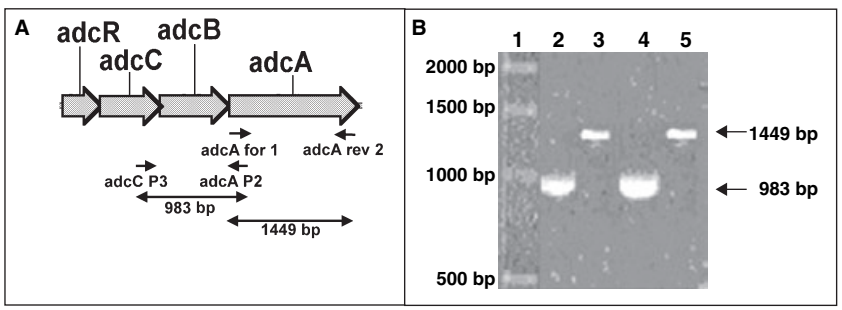

Fig. 1. A) Gene organization of the *adc* operon in *S. gordonii* Challis. Organization of *adc* operon and location of primers that produced an amplicon and their predicted sizes are shown. B) RT-PCR analysis of RNA extracted from *S. gordonii* Challis 2 and *adc* mutants. See Table 1 for all primers used. RT-PCR products using total RNA extracted from *S. gordonii* Challis 2 (lanes 2, 3), *adcC*::*spec*^{R} (lane 4) and *adcB*::*spec*^{R} (lane 5) strains as the template. Lanes: 1, 1kb DNA marker; 2, primers adcC P3 and adcA P2; 3, primers adcA for 1 and adcA rev 2; 4, primers adcC P3 and adcA P2; and 5, primers adcA for 1 and adcA rev 2.

microscope (Leica LaserTechnik GmbH, Heidelberg, Germany) equipped with an argon-krypton laser. Images were collected and analyzed with Image-Pro® Plus computer software (Media Cybernetics, Silver Spring, MD).

Image analysis of each strain was performed using five image stacks acquired from random positions of the flow channel approximately 5 mm from the inlet. Images were acquired at 5-µm intervals down through the biofilm, and therefore the number of images in each stack varied according to the thickness of the biofilm. The data were processed using COMSTAT software (11). The parameters chosen to characterize the biofilm structures were total biomass, average thickness, maximum thickness, and substratum coverage.

Results

The structure of the *S. gordonii adc* operon and its flanking regions was described previously (19) (Fig. 1A). It consists of four genes that encode for AdcR, a putative metal-binding repressor, AdcC, an ATP-binding protein, AdcB, a transmembrane protein and AdcA, a metal binding lipoprotein, in that order. The organization of this operon varies in some streptococcal species in that the *adcA* gene is not always contiguous with the *adc* operon and the AdcA is not always a lipoprotein (19).

The genes encoded by the *adc* operon in *S. gordonii* were inactivated by constructing *adcC*, *adcB*, and *adcA* deletion mutants by PCR ligation mutagenesis (15) using the strategy previously described to construct *adcR* mutants (19). Chromosomal DNA was isolated and analyzed by PCR to confirm that the integration of the $spec^R$ gene in *adcC, adcB, and adcA* genes had occurred as predicted (data not shown).

RT-PCR was performed using RNA isolated from *S. gordonii adcC*::$spec^R$ and *S. gordonii adcB*::$spec^R$ mutants to confirm that the mutants generated were nonpolar. The location of the primers used are shown in Fig. 1A. RT-PCR performed using RNA isolated from *S. gordonii adcC*::$spec^R$ mutant with primers adcC P3 and adcA P2 produced a 983-bp amplicon that spans from *adcC* to *adcA*. RT-PCR using RNA isolated from *S. gordonii adcB*::$spec^R$ with primers adcA for1 and adcA P2 produced a 1449-bp amplicon located within *adcA*. RNA isolated from *S. gordonii* Challis 2 was used as a control to confirm that amplicons of identical size were produced with RT-PCR when identical primer pairs were used (Fig. 1B). These results confirmed that the insertional inactivation of the constructed *adcC*::$spec^R$ and *adcB*::$spec^R$ mutants was nonpolar.

The effects of insertional inactivation of the *adc* operon on competence were examined as previously described (19). Results from transformation of the *S. gordonii* Challis 2, *adcC*::$spec^R$, *adcB*::$spec^R$, and *adcA*::$spec^R$ mutant strains with equal amounts of ligated DNA demonstrated the mutations in individual genes of the *adc* operon resulted in *S. gordonii* mutants that were defective in competence (competence was reduced by 80% in *adcC*:: $spec^R$, 78% in *adcB*::$spec^R$, *and* 60% in *adcA*::$spec^R$ mutants). Therefore, a functional *adc* operon is required for full competence in *S. gordonii*.

Phylogenetic analyses of *S. gordonii* AdcA

AdcA homologs from other streptococci deposited in the DNA databases encoding

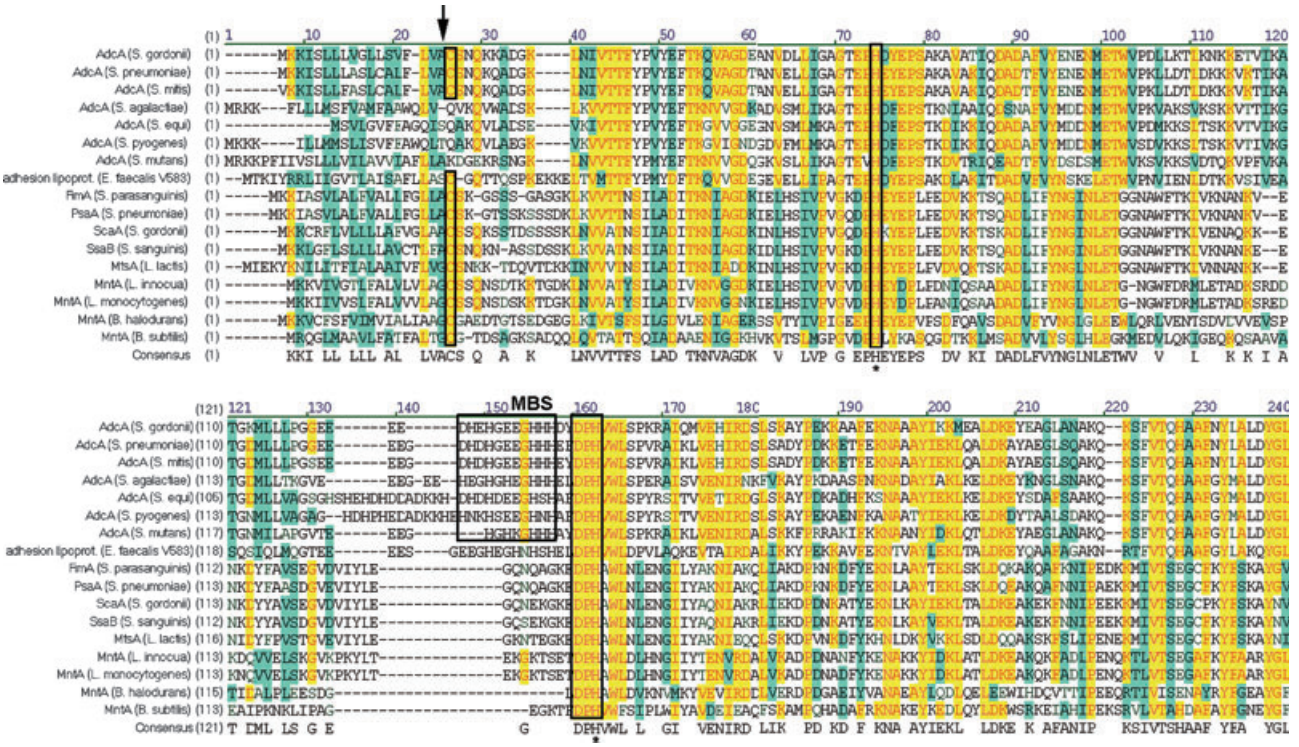

Fig. 2. Alignments of the deduced amino acid sequences of *S. gordonii* AdcA with other streptococcal AdcA homologs. Amino acids that are identical and conserved are highlighted in red in yellow background and black in blue background. The solid vertical arrow indicates the putative position of the prolipoprotein signal processing site of *S. gordonii* AdcA. The putative cysteine residue that is involved in the prolipoprotein signal processing site is boxed after a black arrow. A histidine tract present in AdcA homologs that is proposed to represent a metal-binding site (MBS) is boxed. Two histidine residues that are conserved are boxed and indicated by *. The highly conserved DPH moiety among all species is boxed.

similar proteins were identified using the TBLASTN algorithm (1) and were retrieved from the microbial genome databases (http://www.ncbi.nlm.nih.gov). Phylogenetic analyses demonstrate that *S. gordonii* AdcA is closely related to other ABC-type transporter subclasses belonging to the ABC-type transport system that have now been designated as cluster 9 of metal transporters (6). Amino acid sequence alignments of predicted streptococcal AdcA homologs available in the microbial genome databases indicate that there are distinct differences even though they share high levels of homology (Fig. 2).

Although the majority of these proteins are lipoproteins, there is a distinct subfamily within the AdcA group that does not contain the prolipoprotein signal processing consensus sequence, indicating they are not lipoproteins (Fig. 2). Also the AdcA homologs possess a histidine-rich region (HEHGEEGHHH) that was previously identified as a putative metal binding site (10). Analysis of the crystal structure of pneumococcal PsaA has shown that His67, His139, Glu205 and Asp280 constitute the metal binding site of this protein. This metal-binding site is located between two $(\beta/\alpha)_4$ domains, a characteristic of all known ABC-type binding proteins (16). Similarly in AdcA of *S. gordonii* it can be predicted that His63, His139, His203, and Glu278 are likely to constitute the putative metal binding site of this protein. The DPH moiety, which is an integral part of the metal binding site, is also conserved among all the proteins examined (Fig. 2).

Growth assay

The growth rates and final yields of the *adcR*::*spec*^{R} mutants, *adcC*::*spec*^{R}, *adcB*::*spec*^{R}, and *adcA*::*spec*^{R} were examined and compared to the growth rate and the final yield of *S. gordonii* Challis 2 in THBYE at 37°C under anaerobic conditions (Fig. 3A). The growth rates of *S. gordonii* Challis 2 and *adcR*::*spec*^{R} mutant were similar but *adcC*::*spec*^{R}, *adcB*::*spec*^{R}, and *adcA*::*spec*^{R} mutants grew slower initially. However, the final yields of all of the mutants were found to be similar to that of the parent Challis 2 strain.

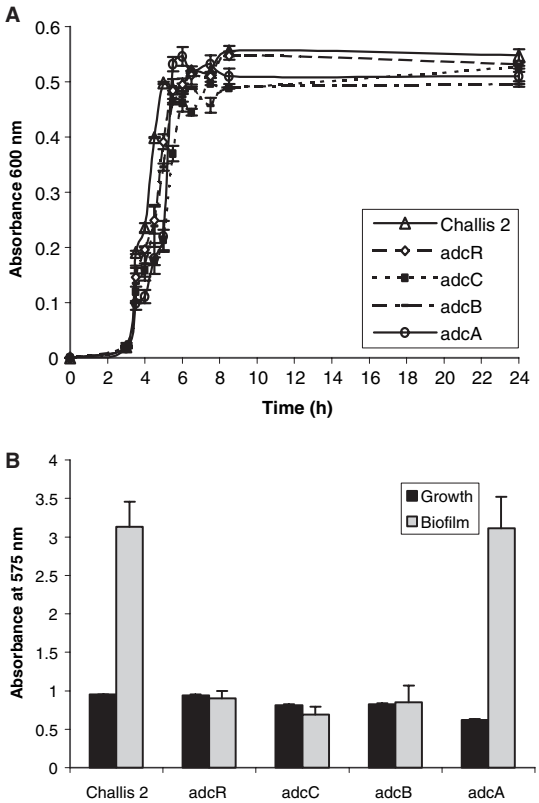

Fig. 3. A) Growth curves of *S. gordonii* Challis 2 and the *adc* mutants in THBYE over 24 h at 37°C under anaerobic conditions. All assays were performed in triplicate, and mean values and standard deviations are shown. B) Bacterial growth and biofilm assay of *S. gordonii* Challis 2 and the *adc* mutants in biofilm medium. Assays were performed using biofilm medium and polystyrene microtiter plates at 37°C under anaerobic conditions. All assays were performed in triplicate, and mean values and standard deviations are shown.

Biofilm formation

The *adc* operon mutants were examined in an *in vitro* biofilm formation assay using polystyrene microtiter plates in biofilm medium (Fig. 3B). Biofilm formation of the *adcC*::*spec*^{R} mutant (A_{575nm} ± standard deviation, 0.69 ± 0.10) and the *adcB*::*spec*^{R} ± mutant (A_{575nm} ± standard deviation, 0.85 ± 0.02) were similar to that of the *adcR*::*spec*^{R} mutant (A_{575nm} ± standard deviation, 0.90 ± 0.01) and were significantly reduced when compared to the Challis 2 strain (A_{575nm} ± standard deviation, 3.13 ± 0.33). In contrast, biofilm formation of the *adcA*::*spec*^{R} mutant (A_{575nm} ± standard deviation, 3.11 ± 0.41) was not significantly different from that of the Challis 2 strain. We have previously shown that insertion of a spectinomycin cassette into *fruR* did not affect biofilm formation of *S. gordonii* (20). This suggests the antibiotic resistance gene did not have a detrimental effect on cell physiology in that the mutant formed a biofilm indistinguishable from the Challis 2 strain.

To clarify the role of *adcA* in biofilm formation, other biofilm assays were performed. Phase-contrast microscopy was used to directly observe the development of *S. gordonii* Challis 2, *adcC*::*spec*^{R}, *adcB*::*spec*^{R}, and *adcA*::*spec*^{R} biofilms on glass coverslips. After 24 h, many more *S. gordonii* Challis 2 had attached to the glass coverslips when compared to the mutant strains *adcC*::*spec*^{R}, *adcB*::*spec*^{R}, and *adcA*::*spec*^{R}, forming biofilms which consisted of multiple layers and thick clusters of densely packed cells. After 24 h, few cells from *adcC*::*spec*^{R}, *adcB*::*spec*^{R}, and *adcA*::*spec*^{R} mutants had attached to the glass surface, forming sparsely distributed small cell clusters (data not shown). The absorbance of the culture medium containing the glass slides were monitored throughout, and no significant differences in growth were observed. These data demonstrate that the *adcC*::*spec*^{R}, *adcB*::*spec*^{R}, and *adcA*::*spec*^{R} mutants were biofilm-defective. Similar to *adcC*::*spec*^{R}, *adcB*::*spec*^{R}, and *adcA*::*spec*^{R} mutants, inactivation of *adcR* has previously been shown to produce a biofilm-defective phenotype on glass surfaces (19).

To confirm these observations, confocal microscopy was carried out to assess whether the mutant strains could form

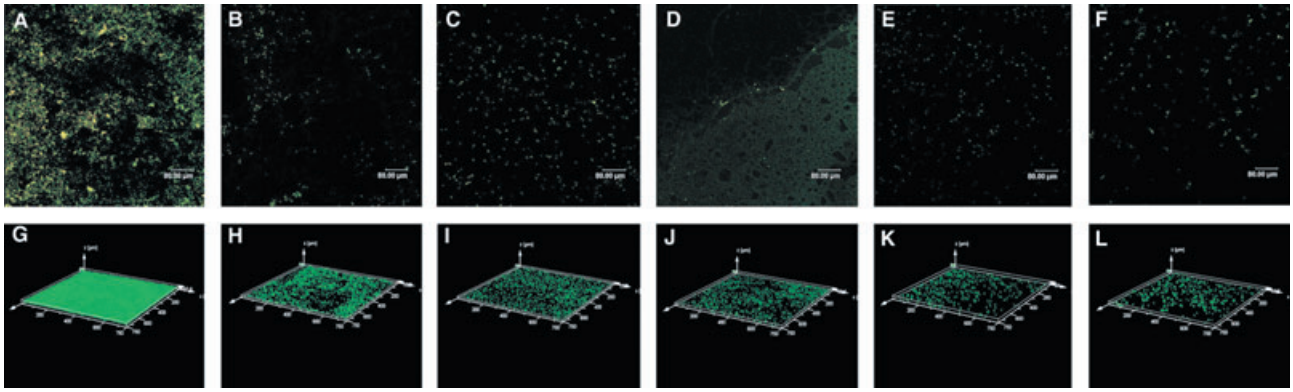

Fig. 4. Confocal scanning laser microscopic analysis of *S. gordonii* biofilms in a flow-cell system. *S. gordonii* Challis 2 (A, G), *adcR*::Tn*917-lac* (B, H), *adcR*::*spec*^{R} (C, I), *adcC*::*spec*^{R} (D, J), *adcB*::*spec*^{R} (E, K), and *adcA*:*spec*^{R} (F, L) strains were grown in biofilm medium in a BST FC71 flow-cell unit (flow rate 180 µl/min; initial inoculum $A_{660} = 0.1$) over 18 h at 37°C. Live cells are stained with Syto-9 (green) and dead cells are stained with propidium iodide (red) and examined by confocal microscopy. A representative image from a set of randomly selected *x–y* stacks (upper panels) and the *x–y–z* perspective (lower panels) are shown for each strain. Bars represent 80 µm.

biofilms in a flow-cell system (18). The biofilms formed by the mutant strains appeared to contain significantly fewer cells than did biofilms formed by Challis 2 (Fig. 4). The Challis 2 biofilm was characterized as a dense, compact biofilm containing thick clusters of cells. In contrast, the mutant biofilms contained sparse clusters made up of a much smaller number of cells.

To determine the spatial architecture of the mutant biofilms vs. the Challis 2 biofilm, quantitative analysis of the biofilms were performed using the COMSTAT program (11); results from the analysis are shown in Table 1. Student's *t*-tests performed to compare values obtained for all five mutant strains with those of the *S. gordonii* Challis 2 strain found significant differences in several of the parameters examined. The total biomass, average thickness, maximum thickness and substratum coverage of the Challis 2 strain was more than twice as high as that was observed with biofilms formed with *adcR*::Tn*917-lac*, *adcR::spec*^{R}, *adcC::spec*^{R}, *adcB::spec*^{R}, and *adcA::spec*^{R} mutants, representing significant quantitative differences.

Discussion

Isolation and characterization of a biofilm-defective mutant of *S. gordonii* with a transposon insertion in an ORF homologous to the *adcR* of *Streptococcus pneumoniae* (9, 10) showed that AdcR plays a role in biofilm formation of *S. gordonii* (19). The *adc* operon of *S. pneumoniae* was previously shown to be involved in metal uptake, specifically zinc (9, 10, 24). The aims of this study were to further investigate the role of the *adcCBA* genes in biofilm formation and competence in *S. gordonii*.

In order to investigate what role the individual genes of the *adc* operon may play in *S. gordonii* biofilm formation, mutations were generated in individual ORFs and biofilm formation by the mutants was examined. Inactivation of *adcR* has been shown previously to result in a biofilm-defective phenotype (19). Inactivation of *adcC* and *adcB* with a *spec*^{R} resulted in a biofilm-defective phenotype. Interestingly, insertional inactivation of *S. gordonii adcA* results in a biofilm-positive phenotype similar to that of *S. gordonii* Challis 2 when examined using the polystyrene microtiter plate biofilm assay. However, when biofilm formation was observed on glass coverslips and in a flow cell, all mutants displayed a biofilm-defective phenotype. Subsequent quantitative analysis demonstrated clear differences between the biofilms formed by Challis 2 and all of the mutants. Although quite useful, these observations demonstrate the need for careful interpretation of data observed with the use of the static microtiter plate assay to study bacterial biofilm formation. All three mutations in the *adc* operon resulted in a defect in competence, suggesting that both competence and biofilm formation are modulated by this operon in *S. gordonii*.

The structure of biofilms may depend on metal ions. An architecturally altered biofilm phenotype has been observed with a *S. gordonii luxS* mutant that is defective in the production of furanosyl borate diester (2), a member of the autoinducer 2 family that elicits responses in numerous bacterial species. Recent studies with *Vibrio cholerae* suggest that calcium present in seawater promotes exopolysaccharide-independent biofilm formation, whereas exopolysachcharide-dependent biofilm occurs in freshwater where the calcium concentration was almost 20 times lower (14).

These results suggest a potentially interesting phenomenon that acquisition of trace elements may act as environmental address signals for bacterial differentiation during bacterial biofilm formation and maturation. Unlike other signals such as pH, osmolarity, and oxygen tension, which are subject to abrupt, sudden changes in an environment by other members of bacterial consortia during cometabolism, trace

Table 1. COMSTAT analysis of confocal scanning laser microscopy images of biofilms formed by S. gordonii in a flow-cell system

Strain	Total biomass ($\mu m^3/\mu m^2$)	Average thickness (µm)	Maximum thickness (µm)	Substratum coverage (%)
Challis 2	0.63 ± 0.15	0.51 ± 0.12	23.92 ± 5.72	3.63 ± 1.11
adcR::Tn*917-lac*	0.27 ± 0.03	0.19 ± 0.03	11.16 ± 2.12	1.78 ± 0.13
adcR::*spec*^{R}	0.30 ± 0.04	0.21 ± 0.04	12.28 ± 2.30	2.06 ± 0.45
adcC::*spec*^{R}	0.29 ± 0.07	0.20 ± 0.07	11.40 ± 3.55	2.11 ± 0.51
adcB::*spec*^{R}	0.33 ± 0.07	0.25 ± 0.07	14.82 ± 4.36	1.73 ± 0.05
adcA::*spec*^{R}	0.38 ± 0.06	0.28 ± 0.05	15.75 ± 2.22	2.15 ± 0.30

The values shown are the means and standard deviations obtained from image stacks of five different areas of the biofilm after 18 h. Student's *t*-tests were performed to compare the values obtained for each mutant strain with those of the *S. gordonii* Challis 2 strain. All *P*-values were < 0.05.

elements may be less susceptible to dramatic fluctuations. Therefore, in certain ecologic habitats, trace elements might be preferable environmental address signals for bacteria to recognize and respond to during the colonization process. During early bacterial evolution, bacteria must have survived on the earth's crust and evolved in a metal age; thus a variety of metal sensing systems would have evolved. Bacteria have retained and refined their metal-sensing systems during evolution for other physiological processes such as bacterial differentiation associated with the biofilm developmental process. The role of trace elements in biofilm dispersal offers a unique opportunity to prevent or disperse biofilms in industrial settings, as the formation of biofilms on a variety of surfaces in the environment is a significant problem that affects industry as well as medicine.

Acknowledgments

This work was supported by PHS grant RO1-DE13328 from the National Institute of Dental and Craniofacial Research. Special thanks go to Dr. Z. Skobe and Elke Pravda at the Biostructure Core Facility in The Forsyth Institute for assistance with confocal microscopy.

References

1. Altschul SF, Gish W, Miller W, Myers EW, Lipman DJ. Basic local alignment search tool. J Mol Biol 1990: **215**: 403–410.
2. Blehert DS, Palmer RJ Jr, Xavier JB, Almeida JS, Kolenbrander PE. Autoinducer 2 production by *Streptococcus gordonii* DL1 and the biofilm phenotype of a *luxS* mutant are influenced by nutritional conditions. J Bacteriol 2003: **185**: 4851–4860.
3. Bloomquist CG, Reilly BE, Liljemark WF. Adherence, accumulation, and cell division of a natural adherent bacterial population. J Bacteriol 1996: **178**: 1172–1177.
4. Carter G, Wu M, Drummond DC, Bermudez LE. Characterization of biofilm formation by clinical isolates of *Mycobacterium avium*. J Med Microbiol 2003: **52**: 747–752.
5. Chen X, Schauder S, Potier N, Van Dorsselaer A, Pelczer I, Bassler BL, et al. Structural identification of a bacterial quorum-sensing signal containing boron. Nature 2002: **415**: 545–549.
6. Claverys JP. A new family of high-affinity ABC manganese and zinc permeases. Res Microbiol 2001: **152**: 231–243.
7. Costerton JW, Lewandowski Z, Caldwell DE, Korber DR, Lappin-Scott HM. Microbial biofilms. Annu Rev Microbiol 1995: **49**: 711–745.
8. Costerton JW, Stewart PS, Greenberg EP. Bacterial biofilms: a common cause of persistent infections. Science 1999: **284**: 1318–1322.
9. Dintilhac A, Alloing G, Granadel C, Claverys JP. Competence and virulence of *Streptococcus pneumoniae*: Adc and PsaA mutants exhibit a requirement for Zn and Mn resulting from inactivation of putative ABC metal permeases. Mol Microbiol 1997: **25**: 727–739.
10. Dintilhac A, Claverys JP. The *adc* locus, which affects competence for genetic transformation in *Streptococcus pneumoniae*, encodes an ABC transporter with a putative lipoprotein homologous to a family of streptococcal adhesins. Res Microbiol 1997: **148**: 119–131.
11. Heydorn A, Nielsen AT, Hentzer M, Sternberg C, Givskov M, Ersboll BK, et al. Quantification of biofilm structures by the novel computer program COMSTAT. Microbiology 2000: **146**: 2395–2407.
12. Horsburgh MJ, Wharton SJ, Karavolos M, Foster SJ. Manganese: elemental defence for a life with oxygen? Trends Microbiol 2002: **10**: 496–501.
13. Jakubovics NS, Jenkinson HF. Out of iron age: new insights into the critical role of manganese homeostasis in bacteria. Microbiology 2001: **147**: 1709–1718.
14. Kierek K, Watnick PI. Environmental determinants of *Vibrio cholerae* biofilm development. Appl Environ Microbiol 2003: **69**: 5079–5088.
15. Lau PC, Sung CK, Lee JH, Morrison DA, Cvitkovitch DG. PCR ligation mutagenesis in transformable streptococci: application and efficiency. J Microbiol Methods 2002: **49**: 193–205.
16. Lawrence MC, Pilling PA, Epa VC, Berry AM, Ogunniyi AD, Paton JC. The crystal structure of pneumococcal surface antigen PsaA reveals a metal-binding site and a novel structure for a putative ABC-type binding protein. Structure 1998: **6**: 1553–1561.
17. Loo CY, Corliss DA, Ganeshkumar N. *Streptococcus gordonii* biofilm formation: identification of genes that code for biofilm phenotypes. J Bacteriol 2000: **182**: 1374–1382.
18. Loo CY, Mitrakul K, Jaafar S, Gyurko C, Hughes CV, Ganeshkumar N. Role of a *nosX* homolog in *Sptreptococcus gordonii* in aerobic growth and biofilm formation. J Bacteriol 2004: **186**: 8193–8206.
19. Loo CY, Mitrakul K, Voss IB, Hughes CV, Ganeshkumar N. Involvement of the *adc* operon and manganese homeostasis in *Streptococcus gordonii* biofilm formation. J Bacteriol 2003: **185**: 2887–2990.
20. Loo CY, Mitrakul K, Voss IB, Hughes CV, Ganeshkumar N. Involvement of an inducible fructose phosphotransferase operon in *Streptococcus gordonii* biofilm formation. J Bacteriol 2003: **185**: 6241–6254.
21. Mitrakul K, Loo CY, Hughes CV, Ganeshkumar N. The role of a *Streptococcus gordonii* copper-transport-operon, *copYAZ*, in biofilm detachment. Oral Microbiol Immunol 2004: **19**: 395–402.
22. Nyvad B, Kilian M. Comparison of the initial streptococcal microflora on dental enamel in caries-active and in caries-inactive individuals. Caries Res 1990: **24**: 267–272.
23. Palmer RJ Jr, Caldwell DE. A flow-cell for the study of plaque removal and regrowth. J Microbiol Methods 1995: **24**: 171–182.
24. Panina EM, Mironov AA, Gefland MS. Comparative genomics of bacterial zinc regulons: enhanced ion transport, pathogenesis, and rearrangement of ribosomal proteins. PNAS 2003: **100**: 9912–9917.
25. Singh PK, Parsek MR, Greenberg EP, Welsh MJ. A component of innate immunity prevents bacterial biofilm development. Nature 2002: **417**: 552–555.
26. Stoodley P, Sauer K, Davies DG, Costerton JW. Biofilms as complex differentiated communities. Annu Rev Microbiol 2002: **56**: 187–209.
27. Tao L, LeBlanc DJ, Ferretti JJ. Novel streptococcal-integration shuttle vectors for gene cloning and inactivation. Gene 1992: **120**: 105–110.
28. Vats N, Lee SF. Active detachment of *Streptococcus mutans* cells adhered to epon-hydroxylapatite surfaces coated with salivary proteins in vitro. Arch Oral Biol 2000: **45**: 305–314.
29. Vats N, Lee SF. Characterization of a copper-transport, *copYAZ*, from *Streptococcus mutans*. Microbiology 2001: **147**: 653–662.